The Journal of Immunology

CCR2$^+$ Monocyte-Derived Dendritic Cells and Exudate Macrophages Produce Influenza-Induced Pulmonary Immune Pathology and Mortality

Kaifeng Lisa Lin, Yasushi Suzuki, Hideki Nakano, Elizabeth Ramsburg and Michael Dee Gunn

J Immunol 2008; 180:2562-2572; ;
doi: 10.4049/jimmunol.180.4.2562
http://www.jimmunol.org/content/180/4/2562

The Journal of Immunology is published twice each month by
The American Association of Immunologists, Inc.,
9650 Rockville Pike, Bethesda, MD 20814-3994.

Print ISSN: 0022-1767 Online ISSN: 1550-6606.

CCR2$^+$ Monocyte-Derived Dendritic Cells and Exudate Macrophages Produce Influenza-Induced Pulmonary Immune Pathology and Mortality[1]

Kaifeng Lisa Lin,[†] Yasushi Suzuki,[2]* Hideki Nakano,[3]* Elizabeth Ramsburg,[‡] and Michael Dee Gunn[4]*[†]

Infection with pathogenic influenza virus induces severe pulmonary immune pathology, but the specific cell types that cause this have not been determined. We characterized inflammatory cell types in mice that overexpress MCP-1 (CCL2) in the lungs, then examined those cells during influenza infection of wild-type (WT) mice. Lungs of both naive surfactant protein C-MCP mice and influenza-infected WT mice contain increased numbers of CCR2$^+$ monocytes, monocyte-derived DC (moDC), and exudate macrophages (exMACs). Adoptively transferred Gr-1$^+$ monocytes give rise to both moDC and exMACs in influenza-infected lungs. MoDC, the most common inflammatory cell type in infected lungs, induce robust naive T cell proliferation and produce NO synthase 2 (NOS2), whereas exMACs produce high levels of TNF-α and NOS2 and stimulate the proliferation of memory T cells. Relative to WT mice, influenza-infected CCR2-deficient mice display marked reductions in the accumulation of monocyte-derived inflammatory cells, cells producing NOS2, the expression of costimulatory molecules, markers of lung injury, weight loss, and mortality. We conclude that CCR2$^+$ monocyte-derived cells are the predominant cause of immune pathology during influenza infection and that such pathology is markedly abrogated in the absence of CCR2. ***The Journal of Immunology,*** **2008, 180: 2562–2572.**

The significant mortality of highly pathogenic influenza strains appears to be due to their propensity to induce severe cytokine-mediated immune pathology (1). During the 1918 influenza pandemic, unusually high mortality rates were seen among young healthy adults, and infection was associated with toxemia, hypoxemia, and severe hemorrhagic inflammatory edema of the lungs (1, 2). Infection of animals with a recreated 1918 strain results in severe pulmonary inflammation, increased expression of cytokines and chemokines in the lung tissues, and an aberrant ineffective immune response (3, 4). Humans infected with highly pathogenic avian influenza display high mortality and acute respiratory distress syndrome progressing to respiratory failure, lymphopenia, thrombocytopenia, and reactive hemophagocytic syndrome thought to be due to uncontrolled immune activation (5, 6). A cytokine storm, with unusually high levels of chemokines and cytokines in serum (7) and lungs (8), is often seen and correlates with fatal outcome (9, 10). Widely disseminated viral infection and secondary bacterial pneumonia appear to be rare (5).

The immune pathology of influenza infection has been associated with several specific cytokines. Mice deficient in NO synthase 2 (NOS2)[5] or TNF-α display decreased mortality when infected with mouse-adapted influenza (11–13). This increased survival appears to occur because NOS2 and TNF-α induce significant lung damage, but contribute little to anti-influenza immune responses (14, 15). The source of pathogenic cytokines during influenza infection has not been determined, but development of pulmonary immune pathology during sepsis has been associated with NOS2 production by a bone marrow-derived cell type, and is reduced by macrophage depletion (16, 17). Neutrophils and, to a lesser extent, macrophages have been suggested to cause lung damage during most cases of acute lung injury and acute respiratory distress syndrome (18). In the case of influenza, myeloid infiltrates predominate, and macrophages infected in vitro are a major source of inflammatory cytokines (19–21). The accumulation of monocytes/macrophages in lungs during influenza infection has been associated with the development of lung injury. Influenza-infected CCR2-deficient mice display decreased monocyte/macrophage accumulation, decreased lung damage, and a trend toward decreased mortality, whereas mice lacking CCR5 display increased pulmonary infiltrates and increased lung damage (20). CCR2-deficient mice also display a reduced accumulation of monocytes/macrophages in lungs and reduced lung injury in other inflammatory lung diseases (22–27), suggesting that one or more CCR2$^+$ cell types can induce pulmonary immune pathology. However, the specific cell types and cell migration events responsible for influenza-induced immune pathology and mortality have not been identified.

*Department of Medicine and [†]Department of Immunology, and [‡]Department of Duke Human Vaccine Institute, Duke University Medical Center, Durham, NC 27710

Received for publication June 25, 2007. Accepted for publication November 29, 2007.

The costs of publication of this article were defrayed in part by the payment of page charges. This article must therefore be hereby marked *advertisement* in accordance with 18 U.S.C. Section 1734 solely to indicate this fact.

[1] This work was supported by National Institutes of Health Grants P30ES011961, U54AI057157, and U01AI 074529.

[2] Current address: Chuo-Samaria Hospital, 1-5-4 Tsukishima Chuo-ku, Tokyo 104-0052 Japan.

[3] Current address: Laboratory of Respiratory Biology, National Institute of Environmental Health Sciences, National Institutes of Health, Research Triangle Park, NC 27709.

[4] Address correspondence and reprint requests to Dr. Michael Dee Gunn, Department of Medicine, Division of Cardiology, Box 3547, Durham, NC 27710. E-mail address: michael.gunn@duke.edu

[5] Abbreviations used in this paper: NOS2, inducible NO synthase; AM, alveolar macrophage; BAL, bronchoalveolar lavage; DC, dendritic cell; DI, double intermediate; exMAC, exudate macrophage; HA, hemagglutinin; IcosL, ICOS ligand; int, intermediate; LDH, lactose dehydrogenase; LN, lymph node; MDCK, Madin-Darby canine kidney; moDC, monocyte-derived DC; SPC, surfactant protein C; TCID, tissue culture infectious dose; WT, wild type.

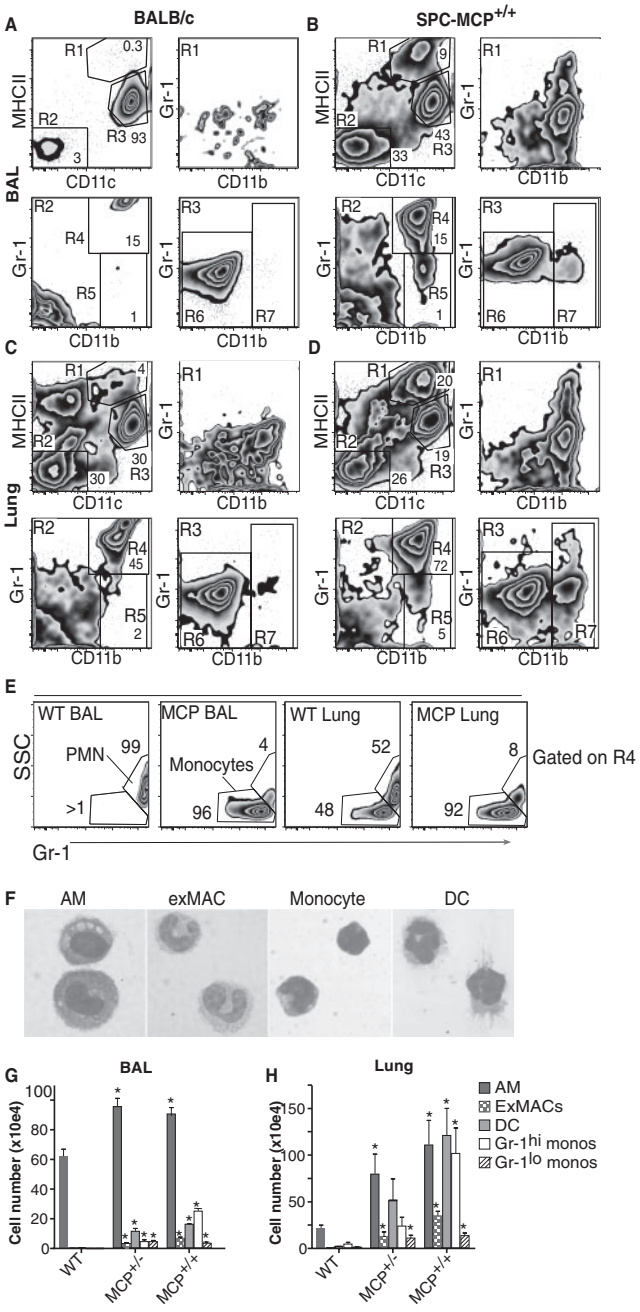

FIGURE 1. Monocytes, DC, AM, and exMACs are increased in the lungs of SPC-MCP mice. *A–D*, Cells from BAL and lung digests were harvested from WT and SPC-MCP mice, and analyzed by flow cytometry. SSC, Side scatter; PMN, polymorphonuclear cell. Results shown are from individual mice representative of three separate experiments. Numbers shown represent the percentage of cells within the gates. *E*, Segregation of Gr-1^{high} monocytes from neutrophils based on Gr-1 vs side scatter (SSC) flow cytometry profiles. Panels display cells with the CD11b^{+}Gr-1^{high} gates of CD11c^{-} MHCII^{-} DN cells (R4). *F*, SPC-MCP lung cells within individual gates were purified by FACS, cytospun, Giemsa stained, and photographed. Original magnification, ×100. *G*, Total cell numbers (per mouse) of individual cell types obtained from lung digests of WT, SPC-MCP$^{+/-}$, and SPC-MCP$^{+/+}$ mice were calculated. Bars represent the mean ± SD for three mice per group. *, $p < 0.05$ compared with WT mice using one-way ANOVA with Dunnett postcomparison test.

Until recently, all macrophages were thought to develop from the progressive maturation of cells along a single lineage of mononuclear phagocytes (28). It is now recognized that at least two

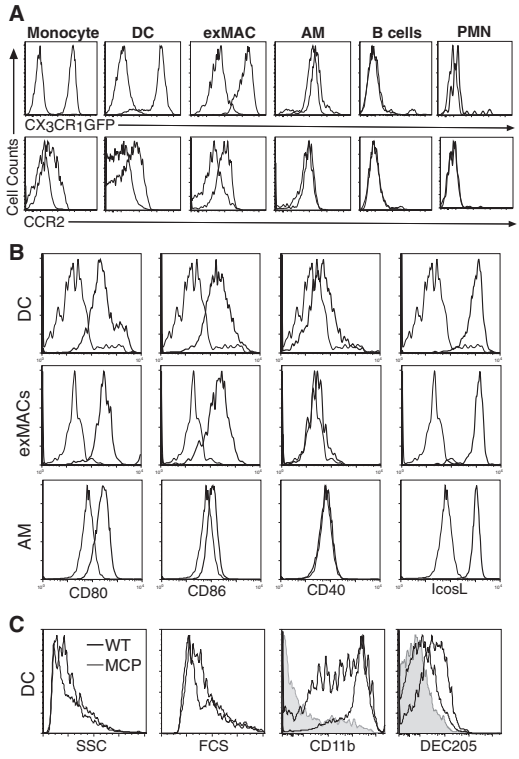

FIGURE 2. Expression levels of selected chemokine receptors and costimulatory molecules on lung cells of SPC-MCP mice. Lung cells were prepared from CX3CR1$^{GFP/+}$ SPC-MCP$^{+/-}$ mice and analyzed by flow cytometry. *A*, Expression of CX3CR1 and CCR2 on individual lung cell types as detected by GFP expression or Ab staining, respectively. PMN, polymorphonuclear cell. *B*, Expression of CD80, CD86, CD40, and IcosL, as detected by Ab staining. Cells were gated as shown in Fig. 1*D*. Faint lines represent staining with IgG control Abs or, for CX3CR1, FITC signal from GFP$^{-/-}$ cells. *C*, Comparison of DC obtained from WT (thick lines) and SPC-MCP (thin lines) mice in side scatter (SSC), forward scatter (FCS), CD11b, and DEC205. Shadow histograms represent control IgG staining. Data are representative of three experiments.

distinct populations of monocytes are present in the circulation (29, 30). Constitutive monocytes, which in mice are CD11b^{+} Gr-1^{-} CCR2^{-} CX3CR1^{high} cells, enter tissues constitutively via the activity of the chemokine receptor CX3CR1 (30). Inflammatory monocytes are CD11b^{+} Gr-1^{high} CCR2^{+} CX3CR1^{int} cells that enter inflamed peripheral and lymphoid tissues via the activity of CCR2 (30, 31). A small population of Gr-1^{int} CCR2^{+} monocytes has also been described (32). Differentiation of monocytes into dendritic cells (DC) in vivo has been well documented (30, 33–35). However, the extent to which monocytes serve as DC precursors under most pathologic conditions remains unclear (36, 37).

In this study, we identify, phenotype, and characterize cell types that accumulate in lungs in response to CCR2 stimulation in mice that constitutively overexpress CCL2 in the lungs (38). We then examine the cell types we identified during influenza infection of wild-type (WT) mice. We find that the majority of inflammatory cells in influenza-infected lungs arise from CCR2^{+} monocytes and include monocyte-derived DC (moDC), exudate macrophages (exMACs), and a transitional cell type. Together, these CCR2^{+} monocyte-derived cells provide the bulk of cytokine production in influenza-infected lungs and are the major cell types responsible for influenza-induced immune pathology, morbidity, and mortality.

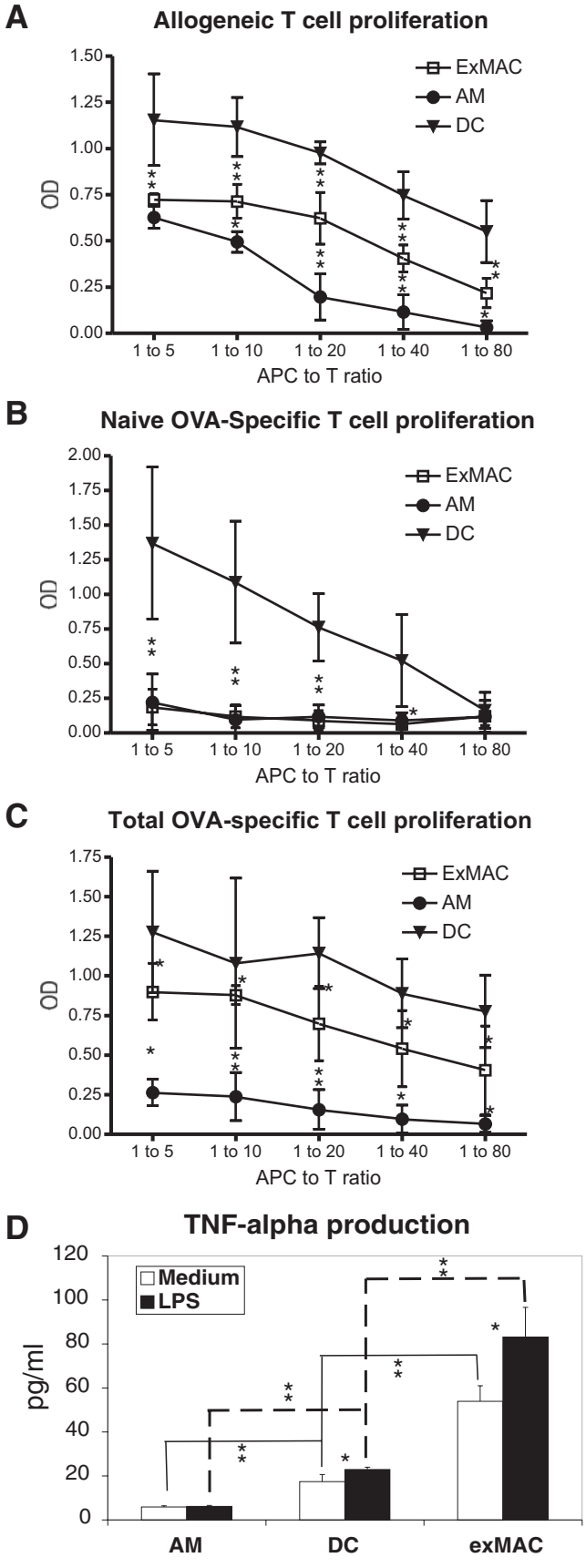

FIGURE 3. T cell stimulation and TNF-α production by DC and macrophages from SPC-MCP mice. *A–C*, DC, AM, and exMACs were purified from the lungs of SPC-MCP mice (BALB/c background) (5 ~ 7 mice pooled) and used as stimulatory cells in assays of T cell proliferation, as measured by BrDU incorporation. Sorted APC purity is between 85 ~ 97.5%, and CD4 T cells purity is 90 ~ 96%. Bars represent the mean ± SD for studies performed in triplicate from two experiments. Response curves were analyzed by linear regression and significant differences between slopes or intercepts determined by ANOVA. *A*, Stimulation of allogeneic (C57BL/6) $CD4^+$ T cells. All response curves are significantly different from each other ($p < 0.0001$). *B*, Stimulation of naive DO11.10 $CD4^+$ T cells in the presence of OVA peptide. Only DC stimulate a significant proliferative response ($p < 0.0001$). *C*, Stimulation of total splenic and LN DO11.10 $CD4^+$ T cells in the presence of OVA peptide. All response curves are significantly different from each other ($p < 0.01$). *D*, DC, AM, and exMACs were purified by FACS from the lungs of SPC-MCP mice and cultured in the presence or absence of LPS. After 48 h, TNF-α levels in the supernatant were measured by ELISA. Bars represent the mean ± SD for studies performed in three experiments. *, $p < 0.05$; **, $p < 0.005$ using ANOVA with Tukey's multiple comparison test.

Materials and Methods

Mice and influenza infection

BALB/c, C57BL/6, and $CCR2^{-/-}$ mice were purchased from Charles River Laboratories or The Jackson Laboratory. Surfactant protein C (SPC)-MCP transgenic mice (38) were backcrossed eight generations onto the BALB/c background. $CX3CR1^{GFP/GFP}$ mice were provided by D. Littman (New York University, New York, NY) and crossed with WT mice to produce $CX3CR1^{+/GFP}$ mice. DO11.10 mice (OVA-specific TCR) and hemagglutinin (HA)-TCR mice (influenza HA-specific TCR) were purchased from The Jackson Laboratory. All mice used for experiments were between 8 and 13 wk old. For flow analysis of flu-infected lung cells, mice were anesthetized by ketamine (100 mg/kg)/xylazine (10 mg/kg) i.p. and then infected with H1N1 influenza virus strain A/Puerto Rico/8/34 (PR8) (provided by Y.-W. He, Duke University, Durham, NC) intranasally (30 μl of 8.9×10^5 tissue culture infectious dose ($TCID_{50}$)/ml virus per mouse). Body weight of infected mice was monitored daily. For mortality, pathology, and viral titer studies, mice were infected with the same virus strain (high dose, 30 μl of 5×10^6 $TCID_{50}$/ml; low dose, 30 μl of 8.5×10^4 $TCID_{50}$/ml), but from a different source (American Type Culture Collection VR-95). All animal experiments were conducted in accordance with National Institutes of Health guidelines and protocols approved by the Animal Care and Use Committee at Duke University.

Bronchoalveolar lavage (BAL) and lung parenchyma cell isolation

BAL cells were collected, as described previously (19). Briefly, tracheas of euthanized mice were cannulated with an 18-gauge angiocath connected to a 1-ml syringe and the lungs were flushed with 0.6~0.8 ml of PBS five times. BAL cells were washed once with PBS. To obtain lung parenchymal cells, lungs were perfused with 3 ml of HBSS-collagenase (1 mg/ml), incubated at 37°C for 30 min, minced, dissociated through a 70-μm mesh strainer, and centrifuged at 450 × *g* at room temperature for 20 min over a 17% metrizamide (Accurate Chemical & Scientific) cushion. Low-density cells were collected, washed in PBS, and subjected to Ab staining.

Flow cytometric analysis

Abs used included anti-NOS2 FITC, anti-I-A/I-E FITC, anti-CD11c PE, and anti-Gr-1 allophycocyanin (all BD Pharmingen); and anti-CD11b allophycocyanin/Cy7, anti-CD11c PECy5.5, anti-CD80 PE, anti-CD86 PE, anti-CD40 PE, anti-ICOS ligand (IcosL) biotin, and streptavidin PE (eBioscience). The anti-CCR2 Ab MC-21 was provided by M. Mack (Klinikum University, Regensburg, Germany). Cells were stained in HBSS containing 10 mM EDTA, 10 mM HEPES, 5% FBS, 5% normal mouse serum, 5% normal rat serum, and 1% Fc block (eBioscience) at 4°C for 30 min; washed three times; and then analyzed using a BD LSRII flow cytometer. For cell sorting, cells were collected and stained as above, and sorted into two to four populations using a BD FACSVantage cell sorter. For morphologic analysis, FACS-purified cell populations from SPC-MCP lungs were cytospun onto microscope slides at 600 rpm for 5 min, stained with Giemsa, and photographed under light microscopy.

T cell proliferation assays

Serial dilutions of FACS-purified AM, DC, and exMACs obtained from SPC-MCP lungs were cultured with 10^5 $CD4^+$ T cells with or without OVA peptide in 96-well plates for 3 days. Allogeneic $CD4^+$ T cells were

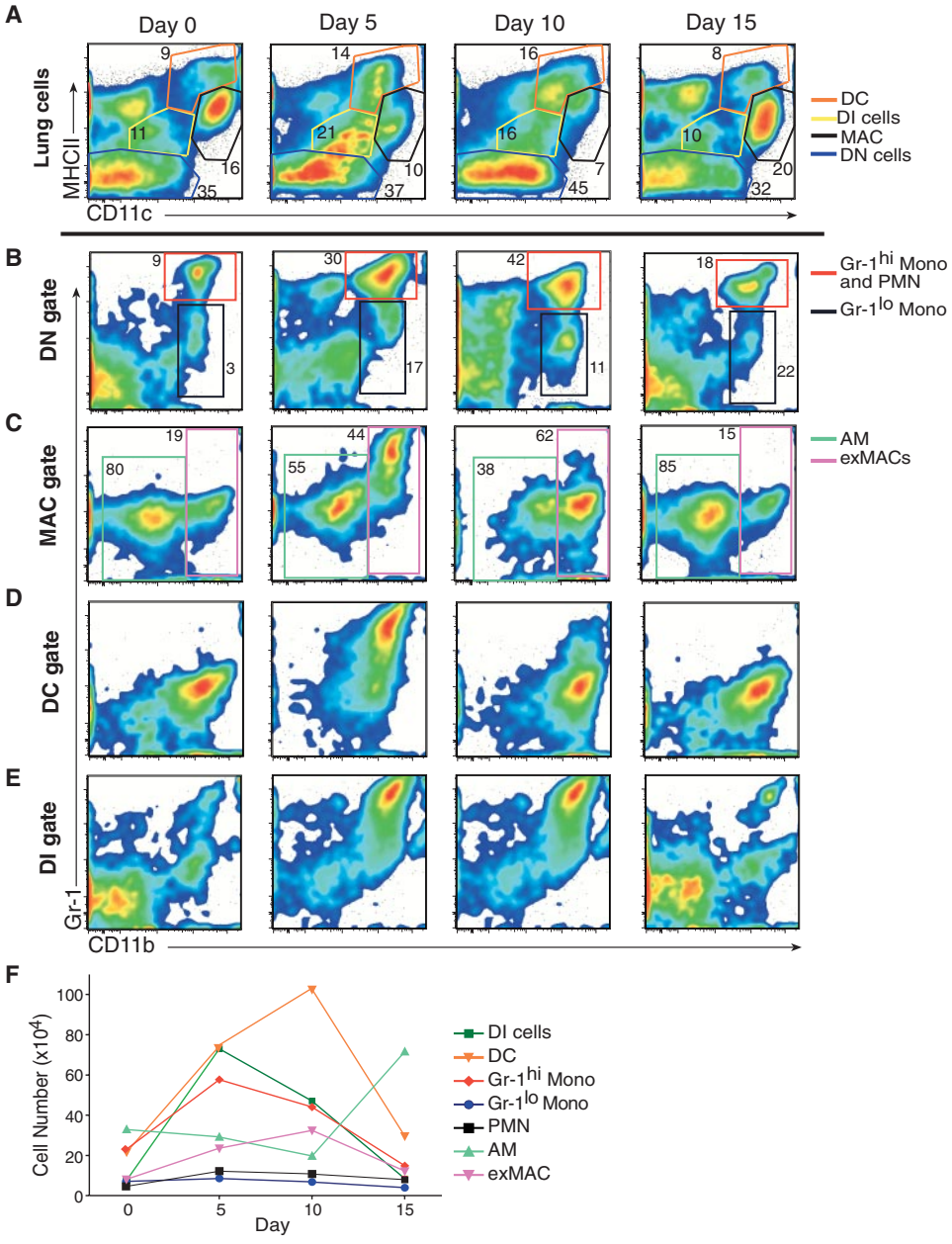

FIGURE 4. Analysis of inflammatory cell types in the lungs of CX3CR1$^{GFP/+}$ mice after infection with influenza virus. CX3CR1$^{GFP/+}$ mice were infected with influenza virus strain A/Puerto Rico/8/34 by intranasal inoculation. At days 0, 5, 10, and 15 after infection, cells obtained from lung digests were analyzed by flow cytometry. *A*, Flow cytometric profiles of total lung cells. Individual gates are color coded according to legend. Results shown are representative of individual mice in three experiments. Numbers shown represent the percentage of cells within the gates. *B–E*, CD11b vs Gr-1 expression on cells within individual gates of panels in Fig. 3*A*. Individual gates are color coded according to legend. *F*, Total cell numbers (per mouse) over time of individual cell types obtained from lung digests of influenza-infected mice. Quantification of neutrophils and their discrimination from other cell types was based on additional analysis of GFP expression (data not shown). Data were derived from pooled samples obtained from two mice and are representative of two experiments for each time point. PMN, Polymorphonuclear cell; MAC, total macrophages.

purified from the spleens and lymph nodes (LN) of C57BL/6 mice using a Lympholyte M gradient, followed by negative selection on a MACS column using biotinylated anti-CD8, anti-CD11b, anti-CD11c, anti-B220, anti-CD16/32, anti-CD19, anti-CD49b, anti-Gr-1, and anti-TER119 Abs (BD Pharmingen), and streptavidin magnetic beads (Miltenyi Biotec). Naive and total OVA-specific CD4$^+$ T cells were derived from the spleens and LN of DO.11.10 mice using the same method, except that naive CD4$^+$ T cells were further purified using a 50–70% Percoll after negative selection. After 3 days of culture, T cell proliferation was measured by BrdU Kit (Roche Applied Science). For CD8 T cell proliferation, 10^4 FACS-purified AM, DC, exMACs, and double-intermediate (DI) cells obtained from flu-infected lungs were cultured with 10^5 CD8$^+$ T cells in 96-well plates for 3 days. CD8 T cells were purified as CD4 T cells, except that anti-CD4 was used instead of anti-CD8 in the negative selection. CD8 T cells were labeled with CFSE (Invitrogen Life Technologies) before being cultured with APCs. Because APCs are not present as distinct populations in infected mice, cells were gated to favor the purity of populations with lower APC activity. Purity of APCs based on strict postsort analysis is as follows: AM, 97%; DI, 85%; DC, 65% (contaminated with DI cells); and exMACs, 68% (contaminated with AM). After 3 days, cells in each well were analyzed by flow cytometry, and CFSE dilution was recorded for CD8$^+$ T cells.

Cytokine expression

FACS-purifed AMs, DCs, and exMACs from SPC-MCP lungs were cultured in 96-well plates in RPMI 1640 with or without LPS for 2 days. Supernatants were assayed for TNF-α concentration using a colorimetric sandwich ELISA kit (R&D Systems). The lowest concentration of standard curve is 15.6 pg/ml. For NOS2 intracellular staining, naive WT and influenza-infected WT and CCR2$^{-/-}$ mice were sacrificed on day 5. BAL and lung parenchyma cells were collected, as above; stained with anti-CD11c, CD11b, I-A/I-E, and Gr-1; and then fixed and permeabilized using BD Cytofix/Cytoperm solution. Cells were then stained with either anti-NOS2 FITC or IgG FITC and analyzed by flow cytometry.

Total BAL protein and lactose dehydrogenase (LDH) activity

Influenza-infected mice were sacrificed on day 6. BAL fluid (3 ml) was obtained, as described above, and separated from BAL cells by centrifugation. The total protein concentration was measured using the Bradford assay reagent (Pierce), according to manufacturer's instruction. LDH activity in BAL fluid was measured using an LDH-based toxicology assay kit (Sigma-Aldrich).

Virus titer measurements

Mice were infected with influenza and sacrificed on day 5. BAL fluid was obtained, as described above. Lung tissues were minced in the same BAL fluid (2 ml), dissociated using a nylon mesh, and centrifuged to remove cells, and the supernatant was collected. Influenza virus titer in lungs and serum was quantified by using standard plaque assay on Madin-Darby canine kidney (MDCK) cells or by determining the $TCID_{50}$ (39). For plaque assays, lung or serum samples were serially diluted in PBS containing Ca^{2+} and Mg^{2+} and 0.1% BSA. Diluted samples were plated on confluent monolayers of MDCK cells and allowed to adsorb for 1 h at 37°C in a tissue culture incubator. After 1 h, inocula were removed and cells were overlayed with 1× MEM containing agar and L-1-tosylamido-2-phenylethyl chloromethyl ketone-treated trypsin (Sigma-Aldrich) at a final concentration of 0.1 μg/ml. Plates were incubated 2 days in a tissue culture incubator (37°C, 5% CO_2) to allow plaques to form. When plaques were clearly visible, agar was removed and the plates were stained with 1% crystal violet in methanol to aid in counting, and then PFU for each sample was determined. To determine $TCID_{50}$, 10× serial dilutions of 0.2-ml aliquots of lung samples were added in triplicate in 96-well plates. A total of 2.5×10^4 MDCK cells was added to each well, and the plates were incubated at 37°C for 5 days. Infected wells were identified by chicken RBC hemagglutination, and $TCID_{50}$ was calculated as described (39).

Statistics

All numerical data are presented as mean ± SD. The comparison between survival curves is performed by log rank test in Prism software. The test is equivalent to the Mantel-Haenszel test. All the other data are analyzed by ANOVA or unpaired Student's *t* tests using Prism software, as indicated in the figure legends.

Results

Identification of cell types recruited to the lung by CCL2

Because the unambiguous identification of pulmonary inflammatory cells during active infection is often difficult, we began these studies by examining the cell types that accumulate in the lung in response to CCL2 overexpression. CCL2 is expressed in the lungs at high levels during influenza infection and has been implicated in the accumulation of monocytes/macrophages in this disease (20, 40, 41). To mimic the robust expression of CCL2 that occurs during influenza infection without the accompanying cell activation and cytopathology, we used SPC-MCP mice, which express high levels of CCL2 under the control of the SPC promoter (38). We and others have shown that large numbers of monocytes and macrophages accumulate in the lungs of SPC-MCP mice, but a detailed phenotypic analysis of the cells recovered has not been performed (38, 42). We now find that the BAL and lungs of SPC-MCP mice contain four distinct cell types in the monocyte-macrophage-DC family. For clarity, we will identify each of these cell types based on the results of these studies, although the identity of some populations was not known at the time these studies were performed.

The first cell type identified in SPC-MCP lungs is alveolar macrophages (AM). Consistent with previous reports (43), AM are autofluorescent CD11c$^+$CD11b$^-$ MHCII^{low} cells that constitute >90% of BAL cells in WT mice (Fig. 1*A*, gate R3). AM are clearly seen in digests of WT lungs (Fig. 1*C*, gate R3) and are increased in number in both the BAL and lungs of SPC-MCP mice (Fig. 1, *B* and *D*, gate R3, and *G*). On cytospins, AM appear as large round cells with abundant vacuolated cytoplasm (Fig. 1*F*).

The second cell type identified in SPC-MCP lungs is DC. These are CD11c$^+$ MHCII^{high} cells that are very infrequent in WT BAL, but are readily apparent in WT lung digests (Fig. 1, *A* and *C*, gate R1). DC are increased in the BAL and markedly increased in the lungs of SPC-MCP mice (Fig. 1, *B* and *D*, gate R1, and *G*). DC from SPC-MCP mice display increased expression of Gr-1 (Fig. 1, *A–D*, gate R1), raising the possibility that these cells recently differentiated from a Gr-1$^+$ precursor population. Morphologically, DC are small cells with vacuolated cytoplasm, a low cytoplasm/nuclear ratio, irregular shaped nuclei, and dendritic processes (Fig. 1*F*).

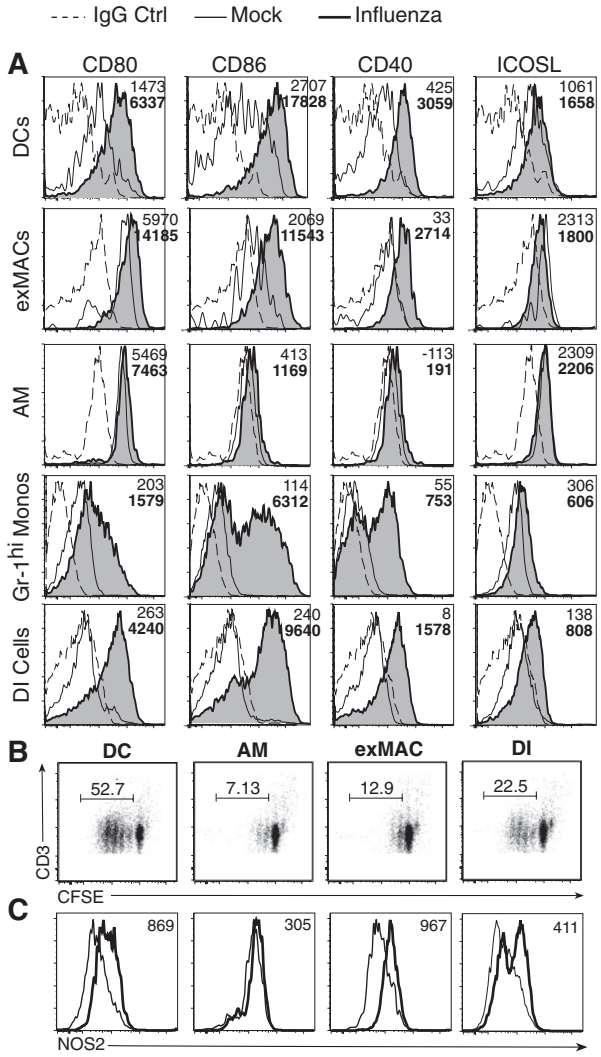

FIGURE 5. Expression of costimulatory molecules, CD8 T cell stimulatory capacity, and NOS2 expression by inflammatory cell types during influenza infection. *A*, Lung cells were obtained from uninfected or day 5 influenza-infected CX3CR1$^{GFP/+}$ mice and analyzed by flow cytometry. Cell populations were gated as in Fig. 4. Staining profiles for the indicated molecules include IgG controls (dashed line), cells from mock-infected mice (thin line), and cells from day 5 infected mice (thick line with shadows). Mean fluorescence intensity above IgG control staining is indicated in plain text for mock controls and in bold text for day 5 infections. Results are representative of three experiments. *B*, HA-TCR (clone 4) CD8 T cells were purified from the spleens of naive mice, labeled with CFSE, and cultured with the indicated APC populations from influenza-infected lungs for 3 days, and CFSE dilution in CD8$^+$ T cells was examined by flow cytometry. Results are representative of two experiments. *C*, Intracellular NOS2 expression in individual cell types obtained from the lungs of WT mice 5 days after influenza infection. Gates shown correspond to those in Fig. 4. Thin lines represent control Ab staining. Mean fluorescence intensity above IgG control is indicated. Results are representative of three experiments.

The third cell type identified in SPC-MCP lungs is inflammatory monocytes. The majority of these CD11c$^-$ MHCII$^-$ CD11b$^+$ monocytes express high levels of Gr-1 (Fig. 1, *B* and *D*, gates R2 and R4), whereas the remainder are Gr-1^{int} (Fig. 1, *B* and *D*, gate R5). Gr-1^{high} monocytes overlap in the expression of several markers with neutrophils (Fig. 1, *A–D*, gate R4), but can be distinguished from the latter based on Gr-1 expression levels and side scatter (Fig. 1*E*) or by expression of CX3CR1

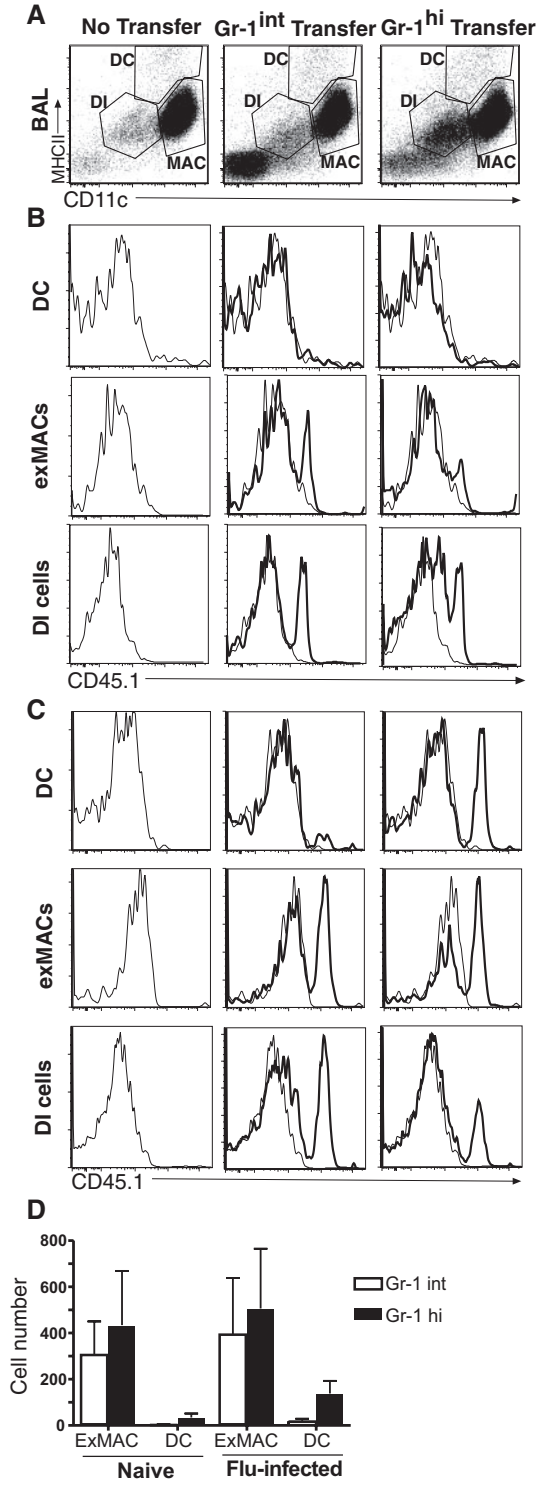

FIGURE 6. Adoptively transferred monocytes develop into DC and exMACs in the lungs of influenza-infected mice. Gr-1$^+$ and Gr-1^{int} monocytes were each purified from the lungs of CD45.1$^+$ SPC-MCP mice (5 ~ 7 mice pooled) and transferred by intratracheal instillation (at 3 ~ 8 × 10^5 cells/mouse) into the lungs of CD45.2$^+$ WT mice. After 24 h, a portion of recipient mice was infected with influenza virus and then sacrificed 1 day later for flow cytometric analysis of BAL cells. *Left column*, PBS only. *Middle column*, Recipients of Gr-1^{int} monocytes. *Right column*, Recipients of Gr-1^{high} monocytes. *A*, Total BAL cells obtained from influenza-infected recipients of no cells (PBS), Gr-1^{int} monocytes, and Gr-1^{high} monocytes. DC, macrophage, and DI gates are shown. *B* and *C*, CD45.1 expression of recipient BAL cells within the DC gate (*upper row*); CD11b$^+$ recipient BAL cells, which represent exMACs, within the macrophage gate (*middle row*); and recipient BAL cells within the DI cell gate (*lower row*). *B*, Naive recipient mice. *C*, Flu-infected recipient mice. Thin lines represent BAL cells of PBS-treated control mice. Results shown are representative of three experiments. *D*, The number of donor CD45.1$^+$ cells in exMAC or DC gates was calculated from three experiments. Bar represents mean ± SD.

(see below). Monocytes are present at very low levels in the BAL and lungs of WT mice (Fig. 1*G*). Lung monocytes display the morphology of monocytes in blood (Fig. 1*F*).

Unlike the above cells, the fourth cell type we find in SPC-MCP lungs has not been clearly identified in previous flow cytometric studies. In both the BAL and lungs of SPC-MCP mice, there appear cells that colocalize with AM in CD11c and MHCII profiles, but are CD11b$^+$ and display less side scatter than AM (Fig. 1, *B* and *D*, gates R3 and R7). These cells proved to be exMACs. On cytospins, exMACs are almost as large as AM, have abundant cytoplasm, and typically have bilobed or kidney-shaped nuclei (Fig. 1*F*).

Molecule expression patterns and activities of inflammatory cells in SPC-MCP mice

To further characterize lung cell types in SPC-MCP mice, we examined expression of costimulatory molecules and the chemokine receptors CX3CR1 and CCR2. As expected, lung monocytes express high levels of CX3CR1 and CCR2, and can thus be easily distinguished from neutrophils, which express neither molecule (Fig. 2*A*). Lung DC are CX3CR1$^+$, predominately CCR2$^+$ (Fig. 2*A*), and express high levels of CD80 and CD86 and low levels of CD40 (Fig. 2*B*). Of interest, DC recovered from the lungs of SPC-MCP mice differ somewhat from DC obtained from WT lungs. Those from SPC-MCP mice display decreased side scatter, decreased forward scatter, decreased expression of DEC205, and increased expression of CD11b (Fig. 2*C*), suggesting that DC in SPC-MCP mice may represent a recruited cell population that differs from resident pulmonary DC. AM express low levels of CD80, but do not express CX3CR1, CCR2, CD86, or CD40 (Fig. 2, *A* and *B*). In contrast, exMACs express CCR2, are uniformly CX3CR1$^+$ (Fig. 2*A*), and express high levels of CD80 and CD86, but little CD40 (Fig. 2*B*), and thus appear more similar to DC than to AM. All lung APC types express high levels of IcosL.

In functional studies, DC obtained from SPC-MCP mice stimulate robust T cell proliferation in all assays of APC activity, including allogeneic T cell proliferation (Fig. 3*A*), naive OVA-specific DO11.10 T cell proliferation (Fig. 3*B*), and total (naive plus memory) DO11.10 T cell proliferation (Fig. 3*C*). AM stimulate only low levels of allogeneic T cell proliferation, and do not stimulate Ag-specific T cell proliferation (Fig. 3, *A–C*). ExMACs stimulate moderate levels of allogeneic T cell proliferation (Fig. 3*A*) and moderate levels of proliferation of total Ag-specific T cells (Fig. 3*C*). However, they do not stimulate the proliferation of naive Ag-specific T cells (Fig. 3*B*), and for this reason are defined in this study as a macrophage, rather than a DC, cell type. For studies of innate immune function, we examined the production of TNF-α by inflammatory cell populations. When cultured, AM purified from SPC-MCP mice produce only background levels of TNF-α, whereas DC produce TNF-α at low levels (Fig. 3*D*). In contrast, exMACs produce significant amounts of TNF-α, which can be further increased by stimulation with LPS. Based on the above assays and previous reports, we identified the major cell types that accumulate in the lungs of SPC-MCP mice as inflammatory monocytes, DC, AM, and exMACs.

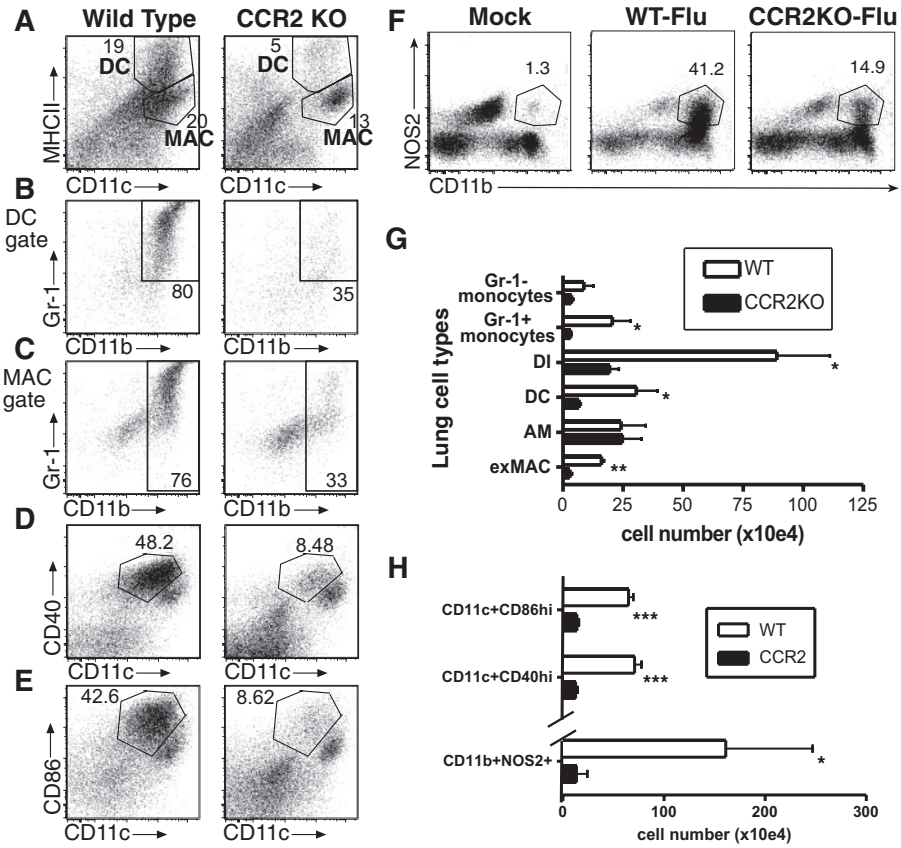

FIGURE 7. Decreased accumulation of inflammatory cells in the lungs of CCR2$^{-/-}$ mice after influenza infection. WT and CCR2$^{-/-}$ mice were infected with influenza virus strain A/Puerto Rico/8/34 by intranasal inoculation. Five days after infection, cells obtained from lung digests were analyzed by flow cytometry (three mice per group). *A*, Flow cytometric profiles of total lung cells. Results shown are for individual mice and representative of three experiments. Numbers shown represent the percentage of cells within the gates. *B*, Cells within the DC gate of panels in *A*. Gr-1^{high} CD1b^{high} DC are indicated. *C*, Cells within the macrophage gate of panels in *A*. CD11b^{high} exMACs are indicated. *D*, Analysis of CD11c vs CD40 staining of total lung cells obtained from influenza-infected mice. *E*, Analysis of CD11c vs CD86 staining of total lung cells obtained from influenza-infected mice. *F*, Intracellular staining of NOS2 in lung cells obtained from WT mice and WT and CCR2$^{-/-}$ mice 5 days after influenza infection. NOS2$^+$ CD11b$^+$ cells are indicated in gate. *G*, Total cell numbers (per mouse) of individual cell types obtained from lung digests of influenza-infected WT and CCR2$^{-/-}$ mice were calculated. Gr-1$^+$ monocytes and neutrophils are distinguished by positive Ly6G staining on neutrophils. *H*, Cell numbers (per mouse) of CD11c$^+$CD86^{high}, CD11c$^+$CD40^{high}, and CD11b$^+$NOS2$^+$ cells obtained from lung digests of influenza-infected WT and CCR2$^{-/-}$ mice. Bars represent the mean ± SD for three mice per group. *, $p < 0.05$; **, $p < 0.005$; ***, $p < 0.0005$ between WT and CCR2 knockout mice using unpaired Student's *t* test.

Pulmonary APC populations in influenza-infected mice

Once we had identified and phenotyped the inflammatory cell types that accumulate in lungs in response to CCL2 overexpression, we sought to determine whether these same cell types also appear in WT mice during infection. We therefore examined lung cell populations in WT BALB/c mice infected with influenza. In initial studies, cell populations appeared in infected WT mice that were similar to those seen in uninfected SPC-MCP mice; however, the very high frequency of CD11b$^+$ Gr-1$^+$ cells found in infected WT mice made it difficult to discriminate neutrophils from other cell types (data not shown). We then examined inflammatory cells in the lungs of influenza-infected CX3CR1$^{GFP/+}$ mice, a model that allows the clear discrimination of GFP$^-$ neutrophils from other CD11b$^+$ Gr-1$^+$ cell types (Fig. 4, GFP gating not shown). Because CX3CR1$^{GFP/+}$ mice are on the C57BL/6 background, we compared inflammatory cell populations in BALB/c and C57BL/6 mice on day 5 of infection and found no significant differences between strains (data now shown). Influenza infection of CX3CR1$^{GFP/+}$ mice results in a marked increase in the number of Gr-1^{high} monocytes in the lungs (Fig. 4, *A* and *B*). Lung Gr-1^{high} monocyte numbers peak at day 5 and return to baseline by day 15 (Fig. 4*F*). Influenza infection also results in both a relative and absolute decrease in lung AM frequency (Fig. 4, *A*, *C*, and *F*). AM numbers reach a nadir at day 10, but recover by day 15 (Fig. 4*F*). Infected mice also display an increase in the number of lung exMACs. Of note, exMACs are almost uniformly Gr-1$^+$ at day 5, but are Gr-1$^-$ at day 10 (Fig. 4*C*), suggesting that these cells have recently differentiated from Gr-1$^+$ monocytes. ExMAC numbers peak at day 10 of infection (Fig. 4*F*). Unexpectedly, the inflammatory cell type that accumulates to the greatest extent during influenza infection is DC (Fig. 4, *A*, *D*, and *F*). As with exMACs, almost all lung DC are Gr-1$^+$ at day 5 after infection, but Gr-1$^-$ at day 10 (Fig. 4*D*), suggesting that these cells arise from Gr-1$^+$ monocytes and thus represent moDC. Intranasal instillation of PBS alone stimulates no significant changes in lung cell populations on day 5 (data not shown).

In addition to the above cells, influenza infection results in the presence of a lung inflammatory cell type that was not observed in SPC-MCP mice. These cells express intermediate levels of both CD11c and MHCII, and are therefore referred to in this study as DI cells (Fig. 4*A*). DI cells express high levels of CD11b, Gr-1, and CX3CR1 (Fig. 4*E*, and data not shown) and appear to represent

Gr-1$^+$ monocytes that are in the process of differentiating into a more mature cell type. Consistent with this, the number of DI cells peaks early in infection (Fig. 4*F*), and DI cells express intermediate levels of CD80, CD86, and CD40 on day 5 of infection (Fig. 5*A*). Day 5 monocytes also display increased expression of CD80, CD86, and CD40. Interestingly, influenza infection results in almost no change in the expression of CD80, CD86, or CD40 by AM (Fig. 5*A*), suggesting that the activation of these cells does not contribute to the inflammatory response. In contrast, DC and exMACs express very high levels of CD80, CD86, and CD40 (Fig. 5*A*).

To determine the capacity of the inflammatory cell types found in the lungs of influenza-infected mice to stimulate influenza-specific T cell responses, we examined the ability of these cells to stimulate the proliferation of influenza HA-specific CD8$^+$ T cells. FACS-purified DC recovered from lungs on day 5 of infection stimulate robust HA-specific T cell proliferation (Fig. 5*B*). DI cells recovered at the same time stimulate moderate levels of HA-specific T cell proliferation (Fig. 5*B*). ExMACs and AM appear to stimulate only low levels of T cell proliferation.

To determine the inflammatory cell populations that express NOS2, an enzyme known to cause lung injury and mortality during influenza infection (12, 15, 44, 45), we examined NOS2 expression by intracellular staining. Both exMACs and DC recovered from lungs on day 5 of infection express NOS2, whereas AM do not (Fig. 5*C*). DI cells display a bimodal distribution of NOS2 expression (Fig. 5*C*).

Direct identification of monocyte-derived cell types

The above findings are consistent with a model in which Gr-1$^+$ inflammatory monocytes enter lungs in response to influenza infection, up-regulate CD11c and MHCII expression to become DI cells, then mature into either exMACs or moDC. To confirm that DI cells, exMACs, and DC arise from monocytes within the lung, we adoptively transferred Gr-1^{high} or Gr-1^{int} monocytes (obtained from the lungs of SPC-MCP mice) via the trachea into the lungs of WT mice and examined the development of these cells in the presence or absence of influenza infection. The phenotype of donor-derived cells in BAL was examined 48 h after transfer and 24 h after infection. Donor cells were uniformly CD11c$^-$ and MHCII$^-$ before transfer (data not shown). In the absence of influenza infection, both Gr-1^{high} and Gr-1^{int} monocytes mature into DI cells and, to a lesser extent, exMACS, but not DC (Fig. 6*B*). In influenza-infected recipients of Gr-1^{int} monocytes, a large proportion of both exMACs and DI cells is donor derived, but few DC are of donor origin (Fig. 6, *A* and *C*). In contrast, donor-derived cells constitute a large proportion of DC, exMACs, and DI cells in infected recipients of Gr-1^{high} monocytes (Fig. 6*C*). Thus, during influenza infection, DI cells, exMACs, and DC can be derived from inflammatory monocytes in the lungs. Influenza infection appears to increase the differentiation of monocytes into moDC (Fig. 6*D*), although this trend does not reach statistical significance ($p = 0.14$).

Inflammatory cell types in CCR2-deficient mice

The above findings strongly suggest that the vast majority of inflammatory cells present in the lungs by day 5 of influenza infection are derived from CCR2$^+$ inflammatory monocytes, and therefore, that the accumulation of these cells is likely to be CCR2 dependent. To test this, we examined lung cell populations in CCR2$^{-/-}$ mice 5 days after influenza infection. We find that CCR2$^{-/-}$ mice display a marked decrease in the accumulation of DC, exMACs, DI cells, and Gr-1$^+$ monocytes during influenza infection (Fig. 7, *A–C* and *G*). Moreover, the populations that are the most reduced in CCR2$^{-/-}$ mice are the CD11b^{high} Gr-1$^+$ subsets of DC and exMACS (Fig. 7, *B* and *C*), and DI cells (Fig. 7*G*).

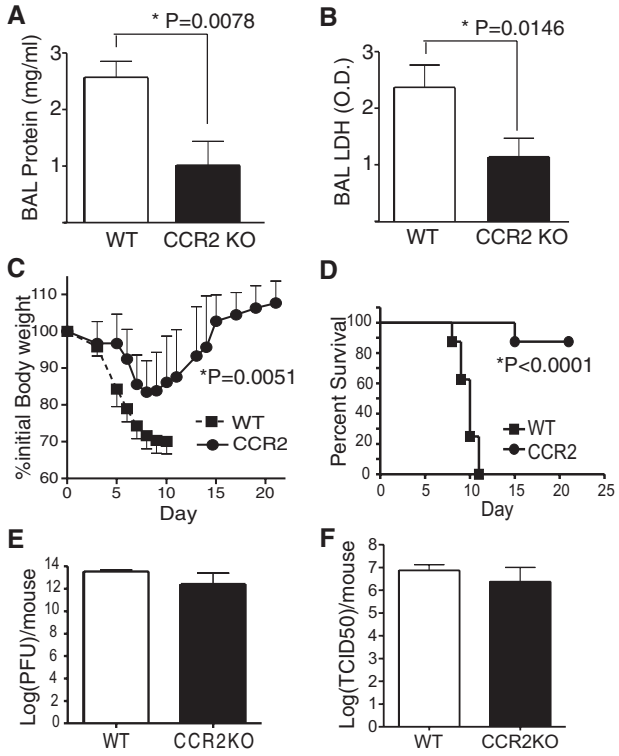

FIGURE 8. Inlfuenza-induced lung injury and weight loss in WT and CCR2$^{-/-}$ mice. WT and CCR2$^{-/-}$ mice were infected with influenza. After 6 days, BAL fluid was assayed for total protein (*A*) and LDH (*B*) activity. Bars represent the mean ± SD for five mice in each group. Value of p is calculated by Student's t test. *C*, Percentage of initial body weight of WT and CCR2$^{-/-}$ mice after influenza infection. Points represent the mean ± SD for eight mice in each group. Value of p is calculated by ANOVA for repeated measures. *D*, Percentage of WT and CCR2$^{-/-}$ mice that survived influenza infection. Total of eight mice for each group. Value of p is calculated by log rank test. *E*, Lungs from WT and CCR2$^{-/-}$ mice were harvested at day 5 after influenza infection, and viral titers were determined by measuring for PFU in total lungs of each mouse. *F*, Lungs from WT and CCR2$^{-/-}$ mice were harvested at day 8 after influenza infection, and viral titers were determined by determining $TCID_{50}$ in total lungs of each mouse. Bars represent the mean ± SD for five mice in each group. Value of p is calculated by Student's t test.

These are also the cell types that express the highest levels of CD86 and CD40, resulting in a marked decrease in cells expressing these costimulatory molecules in infected CCR2$^{-/-}$ mice (Fig. 7, *D*, *E*, and *H*). The frequency of cells expressing NOS2 is also dramatically decreased in CCR2$^{-/-}$ mice (Fig. 7, *F* and *H*). Overall, the accumulation of DC, exMACs, and DI cells during influenza infection is reduced by ~80% in CCR2$^{-/-}$ mice (Fig. 7*G*).

CCR2-dependent influenza-induced pathology and mortality

The finding that CCR2-deficient mice display marked reductions in inflammatory cell numbers and the frequency of cells expressing immune stimulatory molecules and NOS2 suggested that these mice would be protected from influenza-induced immune pathology. We therefore compared markers of influenza-induced lung injury and morbidity between CCR2$^{-/-}$ and WT mice. On day 6 after high dose of virus inoculation, total protein concentration and LDH activity in BAL fluid are both significantly decreased in CCR2$^{-/-}$ relative to WT mice (Fig. 8, *A* and *B*). CCR2$^{-/-}$ mice also display a significant decrease in weight loss after influenza infection (Fig. 8*C*). This decrease in weight loss is highly reproducible. In studies examining other endpoints, WT mice average

19.2% weight loss on day 6 of influenza infection vs 8.3% for CCR2$^{-/-}$ mice ($n = 14$, $p = 0.0004$ by Mann-Whitney U test). Most strikingly, CCR2$^{-/-}$ mice display an 89% decrease in influenza-induced mortality after high-dose influenza infection (Fig. 8*D*). Importantly, this decrease in morbidity and mortality was not associated with an increase in viral titers or dissemination. Five days after a high-dose infection, influenza titers in lungs are slightly, but not significantly, lower in CCR2$^{-/-}$ than in WT mice (Fig. 8*E*), and virus is not detected in the blood of either group (data not shown). To examine viral titers at later time points, we performed low-dose infections. Eight days after low-dose infection, titers are again slightly lower in the lungs of CCR2$^{-/-}$ mice (Fig. 8*F*) and are undetectable in both groups on day 10. These results strongly suggest that the CCR2-dependent migration of monocytes and the development of monocyte-derived inflammatory cells in the lung are largely responsible for the lung injury and subsequent morbidity and mortality that occur during influenza infection.

Discussion

Infection with influenza virus is known to cause significant pulmonary immune pathology. Cell types implicated in this process include neutrophils, activated AM, and macrophages that arise from newly recruited monocytes (18). In this study, we demonstrate that inflammatory monocyte-derived DC and macrophages are the primary cell types responsible for the lung injury, morbidity, and mortality that occur during murine influenza infection. This conclusion is based on several findings. First, during influenza infection, CCR2 deficiency results in marked reductions in weight loss and mortality. This reduced mortality is associated with significant decreases in pulmonary inflammation, TNF-α- and NOS2-producing cells, and with two indices of lung injury, strongly suggesting a causal relationship between monocyte infiltration, pulmonary immune pathology, and mortality. At the same time, influenza infection results in a decrease in AM numbers with little or no increase in costimulatory molecule expression, Ag-presenting activity, or NOS2 expression by AM, suggesting that the activation of these cells does not make a significant contribution to influenza-induced immune pathology. We cannot rule out the possibility that neutrophils play some role in this process, especially early in the course of infection. However, we find relatively little neutrophil accumulation at the times we examine, and the accumulation that we do observe is not affected by CCR2 deficiency (data not shown). In addition, conditional Mcl-1 knockout mice, in which circulating neutrophil numbers are reduced by ~80% (46), display no changes in weight loss or mortality after influenza infection, despite a 70% reduction in lung neutrophil accumulation (K. Lin, unpublished data).

Influenza infection of CCR2$^{-/-}$ mice has previously been shown to result in decreased histological indices of pulmonary inflammation and pathology, a decreased number of monocytes/macrophages in BAL, and a trend toward decreased mortality (19, 20). In this study, we find a much greater effect of CCR2 deficiency on inflammation and mortality. This is most likely due to our use of higher influenza doses, resulting in greater mortality in WT mice, and our use of flow cytometric analyses of lung cells. Our results are most similar to those obtained in NOS2-deficient mice, which display a striking reduction in pneumonitis and mortality after influenza infection (12). This suggests that NOS2 production may be the predominant mechanism by which monocyte-derived cells induce immune pathology and, consistent with Fig. 7, that monocyte-derived cells are the major source of iNOS during influenza infection.

The magnitude of mortality reduction seen in CCR2$^{-/-}$ mice is surprising, given that CCR2 is required for the control of many pulmonary infections (19, 47–49). However, unlike most other pathogens, influenza virus appears to be resistant to host responses such as NOS2 production, and such responses may only inhibit effective adaptive immune responses (12, 50). Consistent with this, we find that influenza-infected CCR2$^{-/-}$ mice display little or no increase in lung viral titers relative to WT mice and no evidence of viral dissemination. In two previous studies, CCR2 deficiency was found to have no effect on (19) or to increase (20) lung influenza titers. However, in the latter study, titers in BAL rather that lung homogenates were examined. NOS2-deficient mice also display reduced lung viral titers during influenza infection (12).

Our examination of monocyte-derived inflammatory cell types in CCL2 transgenic and influenza-infected WT mice provides a mechanism for the reduced immune pathology seen in CCR2$^{-/-}$ mice. As expected, the major circulating cell type recruited to the lungs in both these models is inflammatory monocytes, which include both Gr-1^{high} and, to a lesser extent, Gr-1^{int} cells (Figs. 1 and 4). This finding is similar to previous results obtained in inflamed skin, peritoneum, and lung, because both Gr-1^{high} and Gr-1^{int} monocytes express CCR2 and have been shown to accumulate at sites of CCL2 expression or administration (30, 32, 51, 52). Upon entering the lung, inflammatory monocytes mature to form what appears to be a transitional cell type (DI cells), increasing their expression of CD11c, MHCII, CD40, and CD86, while continuing to express high levels of Ly-6C. A portion of these cells also expresses NOS2. DI cells appear to continue their differentiation to become either moDC or exMACs. Unexpectedly, differentiation to moDC predominates during influenza infection, because these cells are the largest inflammatory cell population found in influenza-infected lungs. The designation of moDC is based on their high expression of CD11c and MHCII, their transient expression of Ly-6C, their morphology, their capacity to stimulate robust proliferation of naive T cells, and their derivation from adoptively transferred Gr-1^{high} monocytes. MoDC are capable of stimulating influenza-specific T cells, but it is presently unclear whether this contributes to anti-influenza immune response.

The second major mature inflammatory monocyte-derived cell population we find in both SPC-MCP and influenza-infected lungs is exMACs. Our designation of these cells is based on their macrophage-like morphology, their capacity to stimulate memory but not naive T cell proliferation, and their derivation directly from monocytes (Figs. 1*E*, 3, and 6). ExMACs display several phenotypic characteristics of DC, including robust expression of CD11c, CX3CR1, CD80, CD86, and CD40 (Fig. 2). However, they would not be classified as a DC subtype because they do not appear to stimulate the proliferation of naive T cells, and they stimulate little, if any, HA-specific T cell proliferation. ExMACs are a major source of inflammatory cytokines, producing high levels of TNF-α and NOS2 (Figs. 3 and 5).

The finding that monocyte-derived cells are the predominant cause of immune pathology during influenza infection raises the possibility that these cells make a significant contribution to other types of acute lung injury. Cells similar to moDC and/or exMACs have been described in several types of pulmonary inflammation, including bleomycin treatment (53), overexpression of GM-CSF (54), and intratracheal instillation of heat-killed *Listeria monocytogenes* (55). It is thus conceivable that inhibition of CCR2 would provide a means to reduce lung injury in several types of pulmonary inflammation. This possibility may be limited to noninfectious causes of lung injury or to infections such as influenza, in which monocyte-derived cells do not significantly contribute to the control of infection. Whether CCR2 inhibition

will have the same effect as CCR2 deficiency or would lead to other adverse effects, such as an increase in secondary bacterial infections, remains to be determined.

Acknowledgments

We thank Drs. Wei Jai and You-Wen He for providing us with influenza virus; Dr. Matthias Mack for the anti-CCR2 mAb; Dr. Dan Littman for CX3CR1$^{GFP/+}$ mice; John Whitesides, Patti McDermott, and Danielle King of Duke Human Vaccine Institute Flow Cytometry facility for their excellent technical assistance; and Keiko Nakano for mouse colony management.

Disclosures

The authors have no financial conflict of interest.

References

1. Doherty, P. C., S. J. Turner, R. G. Webby, and P. G. Thomas. 2006. Influenza and the challenge for immunology. *Nat. Immunol.* 7: 449–455.
2. Patterson, S. 1920. The pathology of influenza in France. *Med. J. Aust.* 1: 207–210.
3. Tumpey, T. M., C. F. Basler, P. V. Aguilar, H. Zeng, A. Solorzano, D. E. Swayne, N. J. Cox, J. M. Katz, J. K. Taubenberger, P. Palese, and A. Garcia-Sastre. 2005. Characterization of the reconstructed 1918 Spanish influenza pandemic virus. *Science* 310: 77–80.
4. Kobasa, D., S. M. Jones, K. Shinya, J. C. Kash, J. Copps, H. Ebihara, Y. Hatta, J. H. Kim, P. Halfmann, M. Hatta, et al. 2007. Aberrant innate immune response in lethal infection of macaques with the 1918 influenza virus. *Nature* 445: 319–323.
5. Beigel, J. H., J. Farrar, A. M. Han, F. G. Hayden, R. Hyer, M. D. de Jong, S. Lochindarat, T. K. Nguyen, T. H. Nguyen, T. H. Tran, et al. 2005. Avian influenza A (H5N1) infection in humans. *N. Engl. J. Med.* 353: 1374–1385.
6. Chotpitayasunondh, T., K. Ungchusak, W. Hanshaoworakul, S. Chunsuthiwat, P. Sawanpanyalert, R. Kijphati, S. Lochindarat, P. Srisan, P. Suwan, Y. Osotthanakorn, et al. 2005. Human disease from influenza A (H5N1), Thailand, 2004. *Emerg. Infect. Dis.* 11: 201–209.
7. Peiris, J. S., W. C. Yu, C. W. Leung, C. Y. Cheung, W. F. Ng, J. M. Nicholls, T. K. Ng, K. H. Chan, S. T. Lai, W. L. Lim, et al. 2004. Re-emergence of fatal human influenza A subtype H5N1 disease. *Lancet* 363: 617–619.
8. Uiprasertkul, M., P. Puthavathana, K. Sangsiriwut, P. Pooruk, K. Srisook, M. Peiris, J. M. Nicholls, K. Chokephaibulkit, N. Vanprapar, and P. Auewarakul. 2005. Influenza A H5N1 replication sites in humans. *Emerg. Infect. Dis.* 11: 1036–1041.
9. De Jong, M. D., C. P. Simmons, T. T. Thanh, V. M. Hien, G. J. Smith, T. N. Chau, D. M. Hoang, N. V. Chau, T. H. Khanh, V. C. Dong, et al. 2006. Fatal outcome of human influenza A (H5N1) is associated with high viral load and hypercytokinemia. *Nat. Med.* 12: 1203–1207.
10. Neumann, G., and Y. Kawaoka. 2006. Host range restriction and pathogenicity in the context of influenza pandemic. *Emerg. Infect. Dis.* 12: 881–886.
11. Peper, R. L., and H. Van Campen. 1995. Tumor necrosis factor as a mediator of inflammation in influenza A viral pneumonia. *Microb. Pathog.* 19: 175–183.
12. Karupiah, G., J. H. Chen, S. Mahalingam, C. F. Nathan, and J. D. MacMicking. 1998. Rapid interferon γ-dependent clearance of influenza A virus and protection from consolidating pneumonitis in nitric oxide synthase 2-deficient mice. *J. Exp. Med.* 188: 1541–1546.
13. Jayasekera, J. P., C. G. Vinuesa, G. Karupiah, and N. J. King. 2006. Enhanced antiviral antibody secretion and attenuated immunopathology during influenza virus infection in nitric oxide synthase-2-deficient mice. *J. Gen. Virol.* 87: 3361–3371.
14. Akaike, T., and H. Maeda. 2000. Nitric oxide and virus infection. *Immunology* 101: 300–308.
15. Davis, I., and S. Matalon. 2001. Reactive species in viral pneumonitis: lessons from animal models. *News Physiol. Sci.* 16: 185–190.
16. Razavi, H. M., L. Wang, S. Weicker, G. J. Quinlan, S. Mumby, D. G. McCormack, and S. Mehta. 2005. Pulmonary oxidant stress in murine sepsis is due to inflammatory cell nitric oxide. *Crit. Care Med.* 33: 1333–1339.
17. Farley, K. S., L. F. Wang, H. M. Razavi, C. Law, M. Rohan, D. G. McCormack, and S. Mehta. 2006. Effects of macrophage inducible nitric oxide synthase in murine septic lung injury. *Am. J. Physiol.* 290: L1164–L1172.
18. Matthay, M. A., and G. A. Zimmerman. 2005. Acute lung injury and the acute respiratory distress syndrome: four decades of inquiry into pathogenesis and rational management. *Am. J. Respir. Cell Mol. Biol.* 33: 319–327.
19. Wareing, M. D., A. Lyon, C. Inglis, F. Giannoni, I. Charo, and S. R. Sarawar. 2007. Chemokine regulation of the inflammatory response to a low-dose influenza infection in CCR2$^{-/-}$ mice. *J. Leukocyte Biol.* 81: 793–801.
20. Dawson, T. C., M. A. Beck, W. A. Kuziel, F. Henderson, and N. Maeda. 2000. Contrasting effects of CCR5 and CCR2 deficiency in the pulmonary inflammatory response to influenza A virus. *Am. J. Pathol.* 156: 1951–1959.
21. Cheung, C. Y., L. L. Poon, A. S. Lau, W. Luk, Y. L. Lau, K. F. Shortridge, S. Gordon, Y. Guan, and J. S. Peiris. 2002. Induction of proinflammatory cytokines in human macrophages by influenza A (H5N1) viruses: a mechanism for the unusual severity of human disease? *Lancet* 360: 1831–1837.
22. Peters, W., J. G. Cyster, M. Mack, D. Schlondorff, A. J. Wolf, J. D. Ernst, and I. F. Charo. 2004. CCR2-dependent trafficking of F4/80^{dim} macrophages and CD11c$^{dim/intermediate}$ dendritic cells is crucial for T cell recruitment to lungs infected with *Mycobacterium tuberculosis*. *J. Immunol.* 172: 7647–7653.
23. Osterholzer, J. J., T. Ames, T. Polak, J. Sonstein, B. B. Moore, S. W. Chensue, G. B. Toews, and J. L. Curtis. 2005. CCR2 and CCR6, but not endothelial selectins, mediate the accumulation of immature dendritic cells within the lungs of mice in response to particulate antigen. *J. Immunol.* 175: 874–883.
24. Belperio, J. A., M. P. Keane, M. D. Burdick, J. P. Lynch III, Y. Y. Xue, A. Berlin, D. J. Ross, S. L. Kunkel, I. F. Charo, and R. M. Strieter. 2001. Critical role for the chemokine MCP-1/CCR2 in the pathogenesis of bronchiolitis obliterans syndrome. *J. Clin. Invest.* 108: 547–556.
25. Moore, B. B., R. Paine III, P. J. Christensen, T. A. Moore, S. Sitterding, R. Ngan, C. A. Wilke, W. A. Kuziel, and G. B. Toews. 2001. Protection from pulmonary fibrosis in the absence of CCR2 signaling. *J. Immunol.* 167: 4368–4377.
26. Gharaee-Kermani, M., R. E. McCullumsmith, I. F. Charo, S. L. Kunkel, and S. H. Phan. 2003. CC-chemokine receptor 2 required for bleomycin-induced pulmonary fibrosis. *Cytokine* 24: 266–276.
27. Hildebrandt, G. C., U. A. Duffner, K. M. Olkiewicz, L. A. Corrion, N. E. Willmarth, D. L. Williams, S. G. Clouthier, C. M. Hogaboam, P. R. Reddy, B. B. Moore, et al. 2004. A critical role for CCR2/MCP-1 interactions in the development of idiopathic pneumonia syndrome after allogeneic bone marrow transplantation. *Blood* 103: 2417–2426.
28. Ross, J. A., and M. J. Auger. 2002. The biology of the macrophage. In *The Macrophage*. B. Burke, and C. E. Lewis, eds. Oxford University Press, Oxford, pp. 1–72.
29. Palframan, R. T., S. Jung, G. Cheng, W. Weninger, Y. Luo, M. Dorf, D. R. Littman, B. J. Rollins, H. Zweerink, A. Rot, and U. H. von Andrian. 2001. Inflammatory chemokine transport and presentation in HEV: a remote control mechanism for monocyte recruitment to lymph nodes in inflamed tissues. *J. Exp. Med.* 194: 1361–1373.
30. Geissmann, F., S. Jung, and D. R. Littman. 2003. Blood monocytes consist of two principal subsets with distinct migratory properties. *Immunity* 19: 71–82.
31. Tsou, C. L., W. Peters, Y. Si, S. Slaymaker, A. M. Aslanian, S. P. Weisberg, M. Mack, and I. F. Charo. 2007. Critical roles for CCR2 and MCP-3 in monocyte mobilization from bone marrow and recruitment to inflammatory sites. *J. Clin. Invest.* 117: 902–909.
32. Sunderkotter, C., T. Nikolic, M. J. Dillon, N. Van Rooijen, M. Stehling, D. A. Drevets, and P. J. Leenen. 2004. Subpopulations of mouse blood monocytes differ in maturation stage and inflammatory response. *J. Immunol.* 172: 4410–4417.
33. Serbina, N. V., T. P. Salazar-Mather, C. A. Biron, W. A. Kuziel, and E. G. Pamer. 2003. TNF/iNOS-producing dendritic cells mediate innate immune defense against bacterial infection. *Immunity* 19: 59–70.
34. Leon, B., M. Lopez-Bravo, and C. Ardavin. 2007. Monocyte-derived dendritic cells formed at the infection site control the induction of protective T helper 1 responses against *Leishmania*. *Immunity* 26: 519–531.
35. Randolph, G. J., K. Inaba, D. F. Robbiani, R. M. Steinman, and W. A. Muller. 1999. Differentiation of phagocytic monocytes into lymph node dendritic cells in vivo. *Immunity* 11: 753–761.
36. Leon, B., M. Lopez-Bravo, and C. Ardavin. 2005. Monocyte-derived dendritic cells. *Semin. Immunol.* 17: 313–318.
37. Gordon, S., and P. R. Taylor. 2005. Monocyte and macrophage heterogeneity. *Nat. Rev. Immunol.* 5: 953–964.
38. Gunn, M. D., N. A. Nelken, X. Liao, and L. T. Williams. 1997. Monocyte chemoattractant protein-1 is sufficient for the chemotaxis of monocytes and lymphocytes in transgenic mice but requires an additional stimulus for inflammatory activation. *J. Immunol.* 158: 376–383.
39. Cottey, R., C. A. Rowe, and B. S. Bender. 2001. Influenza Virus. In *Current Protocols in Immunology.* J. E. Coligan, ed.
40. Sprenger, H., R. G. Meyer, A. Kaufmann, D. Bussfeld, E. Rischkowsky, and D. Gemsa. 1996. Selective induction of monocyte and not neutrophil-attracting chemokines after influenza A virus infection. *J. Exp. Med.* 184: 1191–1196.
41. Wareing, M. D., A. B. Lyon, B. Lu, C. Gerard, and S. R. Sarawar. 2004. Chemokine expression during the development and resolution of a pulmonary leukocyte response to influenza A virus infection in mice. *J. Leukocyte Biol.* 76: 886–895.
42. Winter, C., K. Taut, M. Srivastava, F. Langer, M. Mack, D. E. Briles, J. C. Paton, R. Maus, T. Welte, M. D. Gunn, and U. A. Maus. 2007. Lung-specific overexpression of CC chemokine ligand (CCL) 2 enhances the host defense to *Streptococcus pneumoniae* infection in mice: role of the CCL2-CCR2 axis. *J. Immunol.* 178: 5828–5838.
43. Von Garnier, C., L. Filgueira, M. Wikstrom, M. Smith, J. A. Thomas, D. H. Strickland, P. G. Holt, and P. A. Stumbles. 2005. Anatomical location determines the distribution and function of dendritic cells and other APCs in the respiratory tract. *J. Immunol.* 175: 1609–1618.
44. Akaike, T., Y. Noguchi, S. Ijiri, K. Setoguchi, M. Suga, Y. M. Zheng, B. Dietzschold, and H. Maeda. 1996. Pathogenesis of influenza virus-induced pneumonia: involvement of both nitric oxide and oxygen radicals. *Proc. Natl. Acad. Sci. USA* 93: 2448–2453.
45. Akaike, T., S. Okamoto, T. Sawa, J. Yoshitake, F. Tamura, K. Ichimori, K. Miyazaki, K. Sasamoto, and H. Maeda. 2003. 8-nitroguanosine formation in viral pneumonia and its implication for pathogenesis. *Proc. Natl. Acad. Sci. USA* 100: 685–690.
46. Dzhagalov, I., A. St. John, and Y. W. He. 2007. The antiapoptotic protein Mcl-1 is essential for the survival of neutrophils but not macrophages. *Blood* 109: 1620–1626.

47. Traynor, T. R., W. A. Kuziel, G. B. Toews, and G. B. Huffnagle. 2000. CCR2 expression determines T1 versus T2 polarization during pulmonary *Cryptococcus neoformans* infection. *J. Immunol.* 164: 2021–2027.
48. Peters, W., H. M. Scott, H. F. Chambers, J. L. Flynn, I. F. Charo, and J. D. Ernst. 2001. Chemokine receptor 2 serves an early and essential role in resistance to Mycobacterium tuberculosis. *Proc. Natl. Acad. Sci. USA* 98: 7958–7963.
49. Robben, P. M., M. LaRegina, W. A. Kuziel, and L. D. Sibley. 2005. Recruitment of Gr-1$^+$ monocytes is essential for control of acute toxoplasmosis. *J. Exp. Med.* 201: 1761–1769.
50. Wei, X. Q., I. G. Charles, A. Smith, J. Ure, G. J. Feng, F. P. Huang, D. Xu, W. Muller, S. Moncada, and F. Y. Liew. 1995. Altered immune responses in mice lacking inducible nitric oxide synthase. *Nature* 375: 408–411.
51. Qu, C., E. W. Edwards, F. Tacke, V. Angeli, J. Llodra, G. Sanchez-Schmitz, A. Garin, N. S. Haque, W. Peters, N. van Rooijen, et al. 2004. Role of CCR8 and other chemokine pathways in the migration of monocyte-derived dendritic cells to lymph nodes. *J. Exp. Med.* 200: 1231–1241.
52. Maus, U. A., S. Wellmann, C. Hampl, W. A. Kuziel, M. Srivastava, M. Mack, M. B. Everhart, T. S. Blackwell, J. W. Christman, D. Schlondorff, et al. 2005. CCR2-positive monocytes recruited to inflamed lungs downregulate local CCL2 chemokine levels. *Am. J. Physiol. Lung Cell. Mol. Physiol.* 288: L350–L358.
53. Tager, A. M., A. D. Luster, C. P. Leary, H. Sakamoto, L. H. Zhao, F. Preffer, and R. L. Kradin. 1999. Accessory cells with immunophenotypic and functional features of monocyte-derived dendritic cells are recruited to the lung during pulmonary inflammation. *J. Leukocyte Biol.* 66: 901–908.
54. Wang, J., D. P. Snider, B. R. Hewlett, N. W. Lukacs, J. Gauldie, H. Liang, and Z. Xing. 2000. Transgenic expression of granulocyte-macrophage colony-stimulating factor induces the differentiation and activation of a novel dendritic cell population in the lung. *Blood* 95: 2337–2345.
55. Kradin, R. L., H. Sakamoto, F. I. Preffer, D. Dombkowski, K. M. Springer, and C. P. Leary. 2000. Accumulation of macrophages with dendritic cell characteristics in the pulmonary response to *Listeria*. *Am. J. Respir. Crit. Care Med.* 161: 535–542.